Published in final edited form as:
Genet Med. 2017 April ; 19(4): 386–395. doi:10.1038/gim.2016.126.

Loss-of-function mutations in the X-linked biglycan gene cause a severe syndromic form of thoracic aortic aneurysms and dissections

Josephina A.N. Meester, MSc[1], **Geert Vandeweyer, PhD**[1], **Isabel Pintelon, PhD**[2], **Martin Lammens, MD, PhD**[3], **Lana Van Hoorick**[1], **Simon De Belder**[1], **Kathryn Waitzman, MD**[4], **Luciana Young, MD**[4], **Larry W. Markham, MD**[5], **Julie Vogt, MD**[6], **Julie Richer, MD**[7], **Luc M. Beauchesne, MD**[8], **Sheila Unger, MD**[9], **Andrea Superti-Furga, MD**[9], **Milan Prsa, MD**[10], **Rami Dhillon**[11], **Edwin Reyniers, MSc**[1], **Harry C. Dietz, MD**[12,13], **Wim Wuyts, PhD**[1], **Geert Mortier, MD, PhD**[1], **Aline Verstraeten, PhD**[1], **Lut Van Laer, PhD**[1], and **Bart L. Loeys, MD, PhD**[1]

[1]Center of Medical Genetics, University of Antwerp and Antwerp University Hospital, Antwerp, 2650, Belgium [2]Department of Cell Biology and Histology, University of Antwerp, Antwerp, 2020, Belgium [3]Department of Pathology, University Hospital Antwerp, University of Antwerp, Antwerp, 2610, Belgium [4]Department of Pediatric Cardiology, Ann & Robert H. Lurie Children's Hospital of Chicago, Chicago, IL, 60015, USA [5]Divisions of Pediatric and Adult Cardiology, Vanderbilt University, Nashville, TN, 37232, USA [6]West Midlands Regional Genetics Service, Birmingham Women's NHS Foundation Trust, Birmingham, B15 2TG, United Kingdom [7]Department of Medical Genetics, Children's Hospital of Eastern Ontario, Ottawa, ON, K1H 8L1, Canada [8]Division of Cardiology, University of Ottawa Heart Institute, Ottawa, ON, K1Y 4W7, Canada [9]Service of Medical Genetics, Centre Hospitalier Universitaire Vaudois, Lausanne, 1011, Switzerland [10]Department of Pediatrics, Centre Hospitalier Universitaire Vaudois, Lausanne, 1011, Switzerland [11]The Heart Unit, Birmingham Children's Hospital, Birmingham, B4 6NH, United Kingdom [12]Howard Hughes Medical Institute, Baltimore, MD, 21205, USA [13]McKusick-Nathans Institute of Genetic Medicine, Johns Hopkins University School of Medicine, Baltimore, MD, 21205, USA

Abstract

Purpose—Thoracic aortic aneurysm and dissection (TAAD) is typically inherited in an autosomal dominant manner, but rare X-linked families have been described. So far the only known X-linked gene is *FLNA*, which is associated with the periventricular nodular heterotopia type of Ehlers-Danlos syndrome. However, mutations in this gene only explain a small number of X-linked TAAD families.

Correspondence: Bart L. Loeys (bart.loeys@uantwerpen.be).

Disclosure
The authors declare no conflict of interest.

Europe PMC Funders Author Manuscripts

Methods—We performed targeted resequencing of 368 candidate genes in a cohort of 11 molecularly unexplained Marfan probands. Subsequently, Sanger sequencing of *BGN* in 360 male and 155 female molecularly unexplained TAAD probands was carried out.

Results—We found five individuals with loss-of-function mutations in *BGN*, encoding the small leucine-rich proteoglycan biglycan. The clinical phenotype is characterized by early onset aortic aneurysm and dissection. Other recurrent findings include hypertelorism, pectus deformity, joint hypermobility, contractures and mild skeletal dysplasia. Fluorescent stainings revealed an increase in TGF-β signalling, evidenced by an increase in nuclear pSMAD2 in aortic wall. Our results are in line with prior reports demonstrating that Bgn-deficient male BALB/cA mice die from aortic rupture.

Conclusion—In conclusion, *BGN* gene defects in humans cause an X-linked syndromic form of severe TAAD, associated with preservation of elastic fibres and increased TGF-β signalling.

Keywords

Biglycan; *BGN*; Thoracic aortic aneurysm; Genetics; Marfan Syndrome; Loeys-Dietz Syndrome

Introduction

Thoracic aortic aneurysms (TAA) are often asymptomatic but predispose to aortic dissections, which are associated with high mortality rates.1 Thoracic aortic aneurysms and dissections (TAAD) can be subdivided into syndromic (associated with systemic manifestations) and non-syndromic forms. Most commonly, familial TAADs segregate in an autosomal dominant manner, but rare X-linked families have been described.2 So far, *FLNA* is the only X-linked gene associated with a syndromic form of TAAD, namely the periventricular nodular heterotopia type 1 (PVNH1; also known as the Ehlers-Danlos variant of PVNH, MIM300049). However, *FLNA* only explains a small number of the X-linked TAAD families.3

Marfan syndrome (MFS, MIM154700) is an autosomal dominant connective tissue disorder in which affected individuals present with ocular, skeletal and cutaneous signs besides aneurysm and dissection. Loeys-Dietz syndrome (LDS, MIM609192, MIM610168, MIM613795, MIM614816, MIM615582, and MIM601366) is an aneurysmal connective tissue disorder that can be distinguished from MFS by the unique presence of craniofacial, skeletal, cutaneous, and/or vascular manifestations, prominently including hypertelorism, cleft palate or bifid uvula and arterial tortuosity with aneurysms distant from the aortic root. In addition, aneurysms in individuals with LDS tend to dissect at an earlier age and smaller diameter compared to individuals with MFS.4 Whereas MFS is caused by mutations in *FBN1,* coding for an extracellular matrix (ECM) protein,5 LDS is caused by loss-of-function (LOF) mutations in genes coding for components of the transforming growth factor β (TGF-β) signaling pathway (*TGFBR1/2*, *SMAD2/3*, *TGFB2/3*).6 Recent work has demonstrated that both MFS and LDS lead to dysregulation of the TGF-β signaling pathway.4,7

In the past, biglycan deficiency in male BALB/cA mice was shown to lead to sudden death due to aortic rupture, suggesting that biglycan might be essential for the structural integrity of the aortic wall. Additionally, *BGN* mRNA and protein expression are reduced in individuals with Turner syndrome (45,X),8 who suffer more frequently from vascular anomalies including aortic dissection and rupture.9 Human mutations in *BGN* have not been described in TAAD probands so far.

Here, we report that *BGN* mutations in humans cause an X-linked, severe syndromic form of TAAD, including hypertelorism, pectus deformity, joint hypermobility, contractures and mild skeletal dysplasia.

Materials and Methods

Human participants, DNA and aortic specimens

The study was approved by the appropriate institutional ethics review boards, and the required informed consents were obtained from all participating subjects. Additionally, informed consents for the publication of photos were obtained from the subjects, or legal guardians. DNA of additional affected and unaffected family members was requested whenever considered informative. Aortic specimens from probands 3-III-2 and 5-II-1 as well as from two gender-matched control samples, obtained from deceased individuals who did not suffer from cardiovascular diseases, were at our disposal. As positive controls, we used available aortic specimens from two individuals with LDS (*TGFB3* mutation, p.Asp263His). Fibroblasts were cultured from skin biopsies of probands 4-II-1 and 5-II-1, and two gender-matched control individuals.

Targeted resequencing

We performed targeted resequencing of 368 ECM and TGF-β related genes using the HaloPlex Target Enrichment System (Agilent Technologies, Santa Clara, CA). Samples were paired-end sequenced using 2x100 bp on a HiSeq1500 in high output mode (Illumina, San Diego, CA). Enrichment, data analysis, variant annotation and confirmation of the variants were performed as previously described.10,11 GRCh37 was used as a reference build.

Sanger sequencing and microarray

Sanger sequencing of the seven coding exons of *BGN* (RefSeq transcript NM_001711.3) was performed. The PCR primer sequences and reaction conditions are listed in Table S1. PCR products were bidirectionally sequenced using the BigDye Terminator Cycle Sequencing kit (Applied Biosystems, Carlsbad, CA) and separated on an ABI 3130XL Genetic Analyzer (Applied Biosystems, Carlsbad, CA). Sequences were analyzed using CLC DNA workbench (CLC Bio, Aarhus, Denmark). Microarray analysis was performed using the Illumina HumanCytoSNP12-V2.1 BeadChip (Illumina, San Diego, CA) according to standard protocols. Copy number variant (CNV) analysis was performed using CNV-webstore.12

Cell culture

Skin fibroblasts were cultured in Roswell Park Memorial Institute (RPMI) medium, supplemented with 15% fetal bovine serum (FBS), 1% L-glutamine, 1% sodium pyruvate, 1% Penicillin/Streptomycin and 0,1% Primocin. Experiments were performed at passage 2 to 4. The fibroblasts were incubated with and without puromycin (200 μg/mL) to inhibit nonsense-mediated decay (NMD).

cDNA sequencing and cloning

RNA was extracted from skin fibroblasts (from proband 5-II-1) to identify changes in *BGN* splicing, using the RNeasy mini kit (Qiagen, Valencia, CA), followed by random hexamer cDNA conversion with the Superscript III First-Strand Synthesis kit for RT-PCR (Invitrogen, ThermoFisher Scientific, Waltham, MA). A PCR was performed on the obtained cDNA using the following primers: 5´-CAGAGAGGCTTCTGGGACTT-3´ and 5´-GACGAGGGCGTAGAGGTG-3´. The resulting PCR product was then cloned into One Shot TOP10 cells (ThermoFisher Scientific, Waltham, MA), after which 94 colonies were picked. The different splice products were sequenced with Sanger sequencing.

Histology and immunohistochemistry

Paraffin embedded aortic tissue of affected individuals and control samples was sectioned (5 μm) with the HM340E Microm microtome (ThermoFisher Scientific, Waltham, MA). Histological stainings, including Verhoeff-Van Gieson (VVG) and Masson's Trichrome, were performed using standard protocols.

Fluorescent staining of the aortic tissue with primary antibodies against biglycan (AF2667, 1:40, R&D systems, Minneapolis, MN), decorin (AF143, 1:40, R&D systems, Minneapolis, MN s) and pSMAD2 (04-953, 1:100, Millipore, Billerica, MA) was performed as previously described13, but adapted with the following modifications: the secondary antibodies included chicken-anti-goat Alexa Fluor 488 conjugate (A-21467, 1:200, Life Technologies, ThermoFisher Scientific, Waltham, MA) and goat-anti-rabbit TRITC conjugate (T-2769, 1:200, Life Technologies, ThermoFisher Scientific, Waltham, MA) and treatment with the Fc block Reagent was left out of the protocol. For immunohistochemistry with anti-biglycan and anti-decorin, a pretreatment step with chondroitin ABC lyase (1.25 U/mL, C3667, Sigma-Aldrich, St. Louis, MO) was performed after deparaffinization.14 Confocal images were acquired using the UltraView imaging analysis system (PerkinElmer, Waltham, MA) at 20x and 40x magnification. The number of pSMAD2 positive nuclei was counted in eight fields (40x magnification) for the media and four fields (40x magnification) for the adventitia by five blinded observers.

Results

Identification of *BGN* mutations in syndromic TAAD probands

After targeted resequencing of 368 ECM and TGF-β related genes in a cohort of 11 molecularly unexplained Marfan probands, we identified two individuals with mutations in *BGN*, encoding the ECM small leucine-rich proteoglycan (SLRP) biglycan. In the proband (1-III-1) of family 1 (Figure 1a) we identified a novel nonsense mutation at amino acid

position 2 (c.5G>A, p.Trp2*, ClinVar accession number SCV000266568), while we identified a novel missense variant at the exon-intron boundary of exon 7 (A in AGgt of the donor splice site) in the proband (2-II-1) of family 2 (c.908A>C, p.Gln303Pro, ClinVar accession number SCV000266569). Only minor effect was predicted on splicing (Table S2), but no skin fibroblasts of the proband of family 2 were available to investigate potential aberrant splicing. However, the mutation substitutes a highly conserved amino acid (Figure 1c, Table S2). Subsequently, we performed Sanger sequencing of *BGN* in 360 male and 155 female TAAD probands, negative for mutations in the known TAAD genes.10 As we were unable to amplify exons 2 to 8 of the *BGN* gene in the male probands (3-III-1 en 4-II-1) of family 3 and 4 (Figure 1a), we suspected a partial hemizygous gene deletion. The latter was confirmed by micro-array analysis (Figure 1). In addition, we further delineated these deletions by PCR and Sanger sequencing across the breakpoints. In family 3, we identified a 21 kb deletion spanning chrX:152767424-152787984 (ClinVar accession number SCV000266570), comprising exons 2 to 8 of *BGN*. In family 4, we identified a larger deletion, comprising 28 kb, spanning chrX:152768438-152795976 (ClinVar accession number SCV000266571), but also deleting exons 2 to 8 of *BGN*. In the male proband (5-II-1) of family 5 (Figure 1a), we identified a novel missense mutation at the exon-intron boundary of exon 2, which was predicted to lead to aberrant splicing because the donor splice site was affected (c.238G>A, p.Gly80Ser, ClinVar accession number SCV000266572, Table S2). We subsequently sequenced cDNA from skin fibroblasts of proband 5-II-1 cultured with and without puromycin, a translational inhibitor that will stabilize out of frame transcripts that are normally destined to undergo nonsense-mediated mRNA decay (NMD). Three alternatively spliced products were observed (Figure 2). Of the total amount of *BGN* transcript, only 8% shows normal splicing. The first alternative product (4% representation) incorporates 45 bp of the intron without creating a premature stop codon. The remaining two alternatively spliced products incorporate 111 bp and 368 bp of the intron (with 68% and 20% representation, respectively) and do introduce a premature stop codon leading to NMD. In conclusion, all identified mutations are predicted to lead to a partial or complete loss of function of BGN, either through absence of a functional copy of the gene, through NMD, or through predicted functional changes to protein function (Table S3).

Clinical data

The clinical phenotype of the individuals (Figure 3) with *BGN* mutations is characterized by early onset aortic aneurysm (as early as age 1; 4-II-1) and dissection (earliest at age of 15; 3-II-1) in male probands. In all five families either the aortic root or the more distal ascending aorta was involved. In one family we also observed brain aneurysms in one individual (5-I-2; Figure 1a). Although the mitral and aortic valves were involved in some families (e.g. 2-III-1 and 4-I-2), insufficiency was mild. The cardiovascular phenotype in mutation carrying females ranged from unaffected upon repeated echocardiographic evaluation (3-II-2 and 3-I-2), over aortic root dilatation (4-I-2 and 5-I-2), to death due to aortic dissection (1-II-1). The initial suspected clinical (differential) diagnoses varied between MFS (families 1 and 2), LDS (families 3, 4, 5), Melnick-Needles syndrome and filaminopathy (families 3 and 4). We observed non-specific connective tissue features (e.g. pectus deformities, joint hypermobility/contractures and striae) and more specific manifestations of LDS (e.g. bifid uvula, hypertelorism, and cervical spine instability) in affected individuals. The stature of

the affected patients in this series ranged from short (e.g. 3-III-2 and 4-II-1) to measurements in the normal to high normal range (e.g. 1-III-1, 2-III-1 and 5-II-1) when compared to unaffected family members. Similarly, either long fingers (families 1 and 2) or rather short, broad fingers (families 3 and 4, 5-I-2; Figure 3) were noted. Other unusual features, not typically seen in MFS or LDS, include ventricular dilatation on brain imaging (families 3 and 4), hypertrichosis (family 3), gingival hypertrophy (family 4) and relative macrocephaly (families 3 and 4). There is also evidence of skeletal dysplasia with hip dislocation (families 3 and 4), platyspondyly (family 3), phalangeal dysplasia (families 3 and 4) and dysplastic epiphyses of the long bones (family 3; Figure 3). A detailed clinical description of the five families can be found in the supplemental data.

Structural and functional changes in the aortic wall

In order to investigate collagen and elastic fiber content of the aortic walls, we stained aortic walls from affected (3-III-2 and 5-II-1) and control individuals with Verhoeff-Van Gieson and Trichrome Masson. These stainings revealed a low to normal collagen content, while elastin fibers appeared normal (Figure 4a-h). This is contrast to what is observed in LDS individuals, in whom an increase in collagen production and fragmentation of elastic fibers are typically present.13,15

Next, we fluorescently stained the aortic tissue of the affected probands for biglycan (Figure 4i-l). As expected, no protein expression was detected in proband 3-III-2, since this proband had a deletion of *BGN*. We observed a subtle expression of biglycan in proband 5-II-1, related to the predicted expression of a small amount of wild type (WT) protein. Interestingly, in individuals with LDS (*TGFB3* mutation, p.Asp263His), we specifically observed expression of biglycan in areas with disorganization of the arterial structure. The latter is different to what has been described before in patients with ascending aortic aneurysms of unknown genetic origin.16

In order to investigate whether decorin expression was altered in *BGN* deficient patients, we performed immunohistological stainings of the aortic walls. Decorin is another member of the Class I SLRP, which displays an essential role in the formation and deposition of collagen fibrils and was previously suggested to be able to compensate for biglycan loss.17 We confirmed a focal expression of decorin in the media of the aortic walls of individuals with a BGN mutation (Figure S1), comparable to what has been described in aortic aneurysm patients.16

Since BGN has also been suggested to be a regulator of TGF-β signaling18,19 and since we observed marked phenotypic similarities with MFS and LDS, we hypothesized that an increase in TGF-β signaling could also underlie the phenotype seen in individuals with a *BGN* mutation. Therefore, we stained pSMAD2, a specific marker of activated canonical TGF-β signaling (Figure 4m-p). We observed an increase of pSMAD2 positive nuclei compared to controls, confirming an increase in TGF-β signaling. In addition, a gradient of increased nuclear pSMAD2 staining towards the adventitia was observed in proband 3-III-2 (Figure S2). The increased TGF-β signaling in the media was comparable to the LDS affected individual.

Discussion

The *BGN* gene is located on chromosome Xq28 and encodes the biglycan protein.20 Biglycan belongs to the SLRP Class I proteins and is, together with other proteoglycans such as decorin, mainly involved in ECM assembly and maintenance.21 It consists of a small protein core (~42 kDa),14 which contains 10 leucine-rich repeats (LRR),22 with two tissue specific chondroitin or dermatan-sulfate glycosaminoglycan (GAG) chains attached to two Ser-Gly sites in the N-terminus of the core protein.23,24 Through the core protein and GAG chains, biglycan interacts with many other ECM proteins, including collagen type I, II, III and VI and elastin.25–28 In this manner, biglycan becomes sequestered in the ECM of most organs; its role seems to be not only that of a mechanical link between matrix components, but also that of growth factor binding and regulation of signaling. In healthy individuals, biglycan is expressed by various specialized cell types, including endothelial cells, skeletal myocytes and differentiating keratinocytes.14 It is widely expressed in various tissues throughout the body, including bone, skin, heart, lung and arteries.14,29 In the aorta, biglycan is present in the intima and the media14 but the adventitia is the major site of deposition.17

Due to the suggested structural role of biglycan, we performed histological staining to assess the architecture of the aortic wall. We observed a normal appearance of elastic fibers, and low to normal collagen content in the aortic wall of our probands. This is in contrast to what has been described for MFS and LDS aortic tissues, where an increase in collagen content and an increase in elastic fiber breaks are typically observed.15,30,31 As observed in *bgn*-deficient mice, we hypothesize that proper functioning of biglycan is necessary for correct collagen fibril diameters and lateral association of fibers rather than collagen amount.32

In addition to its structural role, biglycan interacts with several growth factors and cytokines, including TGF-β18,19, to modulate proliferation, migration and differentiation of cells.33 This regulatory function resembles that of fibrillin-1, which also forms a reservoir for latent TGF-β.7 Our results indicate that lack of biglycan increases TGF-β signaling, especially in the adventitia, the major site of biglycan deposition in the aortic wall.17 This may explain why *BGN* deficiency has a more pronounced effect on TGF-β signaling in this layer of the aortic wall.17 Up to now, the upregulation of TGF-β signaling in other syndromic forms of TAAD, like MFS and LDS, has mainly been studied in the media of the aortic wall.15 In the individuals with a *BGN* mutation, we indeed observed a slight increase in TGF-β signaling in the media, however, this increase was significantly more pronounced in the adventitia (Figure S2). The increase in TGF-β signaling is expected to lead to an increased transcription of collagen, but proper collagen fibril assembly may be hampered by biglycan deficiency. Our findings of increased TGF-β signaling are in line with prior observations of enhanced SMAD2 phosphorylation in bgn+/- cardiac fibroblasts.34 The latter induced differentiation into a pro-proliferative myofibroblast phenotype that is rescued by TGF-β neutralizing antibodies. The absence of an aortic phenotype in the pure C57Bl6 *Bgn* deficient mice35 confirms our hypothesis of increased TGF-β signaling as the driving pathogenetic mechanism of the aortic aneurysm development. Indeed, the C57Bl6 mouse background is believed to induce a relative deficiency state for TGF-β signaling and as such attenuates high TGF-β signaling in *Bgn* deficient aortic walls. Only in male BALB/cA mice

biglycan deficiency leads to sudden death from aortic rupture, indicating that biglycan is indeed both structurally and functionally essential for the integrity of the aortic wall.17 The molecular mechanism for the difference between the pure C57Bl6 and the BALB/cA background remains unknown.

As a consequence of the mice studies discussed above, biglycan gene defects were predicted to play a potential role in the pathogenesis of aortic dissection and rupture in humans.17 Yet, this study is the first to report *BGN* mutations in TAAD probands. In *Bgn* knock-out mice, aortic elastic lamella did not display any structural changes,17 similar to the human *BGN* probands. These normal elastic fibers can potentially be explained by the ability of decorin to substitute for biglycan in pathological contexts.17 Decorin is another member of the Class I SLRP, which displays an essential role in the formation and deposition of collagen fibrils and like biglycan, is able to bind tropoelastin, fibrillin-1, and microfibril-associated glycoprotein 1.26,36 However, its expression pattern is somewhat different from biglycan and, depending on the tissue, its synergistic or additive effects with biglycan can differ.37 *Bgn*/*Dcn* double- knock-out mice on a 129Sv/C57BL6 background have been generated in the past, but an aortic phenotype has not been extensively studied.37 As such, it might be interesting to study the aortic phenotype of the *Bgn*/*Dcn* double-KO mice on a BALB/cA background.

In addition to their cardiovascular phenotype, *Bgn* deficient mice have also been reported to show a phenotype characterized by growth failure, reduced bone formation, and age-related severe osteopenia.32 Previous research has indicated that the expression levels of biglycan are potentially related to stature in humans: patients with Turner syndrome have low levels of biglycan and typically display short stature, whereas patients with triple X syndrome present with increased limb length and high levels of biglycan.32 In both family 3 and 4, affected male individuals present short stature (Table 1) and mild skeletal dysplasia (Figure 3b), confirming a role for biglycan in human bone development.

From a clinical perspective, the phenotype of *BGN*-mutated individuals overlaps with LDS and MFS individuals. Typical LDS features in family 3 and 4 include the pronounced hypertelorism, bifid uvula and early onset aortic dissections. The probands of family 1 and 2 were initially diagnosed with MFS but they also display LDS-like features such as hypertelorism. The phenotype of the carrier females ranges from unaffected upon repeated echocardiographic exam (3-II-2 and 3-I-2), over aortic root dilatation (4-I-2 and 5-I-2) to death due to aortic dissection (1-II-1). Overall, the non-cardiovascular characteristics of the females carriers seems milder. To determine whether skewed X-inactivation underlies the difference between affected and unaffected females, we performed X-inactivation experiments using the HUMARA assay.38 The results did not reveal a clear pattern of skewed X-inactivation that could explain the observed difference (data not shown). The phenotypic features in families 3 and 4 seem more pronounced than in the other families. Complete LOF cannot explain this difference between the families, since we also expect a complete LOF in family 1 due to the stop codon at the second amino acid position (even if the first downstream ATG would be used as an alternative start codon, the resulting protein would miss the signal- and the propeptide of biglycan and thus still lead to LOF). However, the deletion occurring in both family 3 and family 4 extends beyond exons 2-8 of *BGN* and

includes a region downstream of the *BGN* gene that contains a CpG-island and in addition, the untranslated region (5'-UTR) of two alternative protein coding transcripts of the downstream gene *ATP2B3*. So far, mutations in *ATP2B3* are linked to an X-linked form of spinocerebellar ataxia39,40 and can therefore not be directly linked to the phenotype of the *BGN* probands. Nonetheless, (intronic) regulatory elements may play a role in the expression of the phenotype and explain the observed difference. The milder phenotype in family 5 could be correlated with 8% residual expression of WT spliced biglycan protein.

In conclusion, our results confirm that *BGN* gene defects in humans cause an X-linked syndromic form of severe TAAD. The identification of mutations in *BGN* contributes to the molecular diagnosis of X-linked TAAD and should therefore be implemented in diagnostics. The signature of increased TGF-β signaling in the aortic walls of the *BGN* deficient patients offers an interesting therapeutic target for TGF-β activity attenuating agents such as angiotensin receptor blockers.

Supplementary Material

Refer to Web version on PubMed Central for supplementary material.

Acknowledgements

We are grateful to the families who participated in this study. We acknowledge Christophe Hermans (CORE, University of Antwerp) and Dominique De Rijck (Department of Cell Biology and Histology, University of Antwerp) for technical support. This research was supported by funding from the University of Antwerp (Lanceringsproject), the Fund for Scientific Research, Flanders (FWO, Belgium, G.0221.12), The Dutch Heart Foundation (2013T093), the Fondation Leducq (MIBAVA – Leducq 12CVD03), and ancillary genetics grant to NIH Marfan losartan study from the National Marfan Foundation. Dr. Loeys is senior clinical investigator of the Fund for Scientific Research, Flanders and holds a starting grant from the European Research Council (ERC-StG-2012-30972-BRAVE). J.A.N.M. is a predoctoral researcher of the Fund for Scientific Research, Flanders (FWO, Belgium).

References

1. Lindsay ME, Dietz HC. Lessons on the pathogenesis of aneurysm from heritable conditions. Nature. May 19; 2011 473(7347):308–316. [PubMed: 21593863]
2. Coady MA, Davies RR, Roberts M, et al. Familial patterns of thoracic aortic aneurysms. Archives of surgery. Apr; 1999 134(4):361–367. [PubMed: 10199307]
3. Sheen VL, Jansen A, Chen MH, et al. Filamin A mutations cause periventricular heterotopia with Ehlers-Danlos syndrome. Neurology. Jan 25; 2005 64(2):254–262. [PubMed: 15668422]
4. Loeys BL, Chen J, Neptune ER, et al. A syndrome of altered cardiovascular, craniofacial, neurocognitive and skeletal development caused by mutations in TGFBR1 or TGFBR2. Nature genetics. Mar; 2005 37(3):275–281. [PubMed: 15731757]
5. Dietz HC, Cutting GR, Pyeritz RE, et al. Marfan syndrome caused by a recurrent de novo missense mutation in the fibrillin gene. Nature. Jul 25; 1991 352(6333):337–339. [PubMed: 1852208]
6. Verstraeten A, Alaerts M, Van Laer L, Loeys B. Marfan Syndrome and Related Disorders: 25 Years of Gene Discovery. Hum Mutat. Feb 26.2016
7. Neptune ER, Frischmeyer PA, Arking DE, et al. Dysregulation of TGF-beta activation contributes to pathogenesis in Marfan syndrome. Nature genetics. Mar; 2003 33(3):407–411. [PubMed: 12598898]
8. Geerkens C, Vetter U, Just W, et al. The X-chromosomal human biglycan gene BGN is subject to X inactivation but is transcribed like an X-Y homologous gene. Hum Genet. Jul; 1995 96(1):44–52. [PubMed: 7607653]

9. Lin AE, Lippe BM, Geffner ME, et al. Aortic dilation, dissection, and rupture in patients with Turner syndrome. J Pediatr. Nov; 1986 109(5):820–826. [PubMed: 3772661]
10. Proost D, Vandeweyer G, Meester JA, et al. Performant Mutation Identification Using Targeted Next-Generation Sequencing of 14 Thoracic Aortic Aneurysm Genes. Hum Mutat. Aug; 2015 36(8):808–814. [PubMed: 25907466]
11. Vandeweyer G, Van Laer L, Loeys B, Van den Bulcke T, Kooy RF. VariantDB: a flexible annotation and filtering portal for next generation sequencing data. Genome medicine. 2014; 6(10):74. [PubMed: 25352915]
12. Vandeweyer G, Reyniers E, Wuyts W, Rooms L, Kooy RF. CNV-WebStore: Online CNV Analysis, Storage and Interpretation. BMC Bioinformatics. Jan 5.2011 12(1):4. [PubMed: 21208430]
13. Bertoli-Avella AM, Gillis E, Morisaki H, et al. Mutations in a TGF-beta ligand, TGFB3, cause syndromic aortic aneurysms and dissections. Journal of the American College of Cardiology. Apr 7; 2015 65(13):1324–1336. [PubMed: 25835445]
14. Bianco P, Fisher LW, Young MF, Termine JD, Robey PG. Expression and localization of the two small proteoglycans biglycan and decorin in developing human skeletal and non-skeletal tissues. J Histochem Cytochem. Nov; 1990 38(11):1549–1563. [PubMed: 2212616]
15. Maleszewski JJ, Miller DV, Lu J, Dietz HC, Halushka MK. Histopathologic findings in ascending aortas from individuals with Loeys-Dietz syndrome (LDS). The American journal of surgical pathology. Feb; 2009 33(2):194–201. [PubMed: 18852674]
16. Gomez D, Al Haj Zen A, Borges LF, et al. Syndromic and non-syndromic aneurysms of the human ascending aorta share activation of the Smad2 pathway. J Pathol. May; 2009 218(1):131–142. [PubMed: 19224541]
17. Heegaard AM, Corsi A, Danielsen CC, et al. Biglycan deficiency causes spontaneous aortic dissection and rupture in mice. Circulation. May 29; 2007 115(21):2731–2738. [PubMed: 17502576]
18. Hildebrand A, Romaris M, Rasmussen LM, et al. Interaction of the small interstitial proteoglycans biglycan, decorin and fibromodulin with transforming growth factor beta. Biochem J. Sep 1; 1994 302(Pt 2):527–534. [PubMed: 8093006]
19. Kolb M, Margetts PJ, Sime PJ, Gauldie J. Proteoglycans decorin and biglycan differentially modulate TGF-beta-mediated fibrotic responses in the lung. American journal of physiology. Lung cellular and molecular physiology. Jun; 2001 280(6):L1327–1334. [PubMed: 11350814]
20. McBride OW, Fisher LW, Young MF. Localization of PGI (biglycan, BGN) and PGII (decorin, DCN, PG-40) genes on human chromosomes Xq13-qter and 12q, respectively. Genomics. Feb; 1990 6(2):219–225. [PubMed: 1968422]
21. Halper J. Proteoglycans and diseases of soft tissues. Adv Exp Med Biol. 2014; 802:49–58. [PubMed: 24443020]
22. Iozzo RV. The family of the small leucine-rich proteoglycans: key regulators of matrix assembly and cellular growth. Crit Rev Biochem Mol Biol. 1997; 32(2):141–174. [PubMed: 9145286]
23. Choi HU, Johnson TL, Pal S, Tang LH, Rosenberg L, Neame PJ. Characterization of the dermatan sulfate proteoglycans, DS-PGI and DS-PGII, from bovine articular cartilage and skin isolated by octyl-sepharose chromatography. The Journal of biological chemistry. Feb 15; 1989 264(5):2876–2884. [PubMed: 2914936]
24. Roughley PJ, White RJ. Dermatan sulphate proteoglycans of human articular cartilage. The properties of dermatan sulphate proteoglycans I and II. Biochem J. 1989 Sep 15; 262(3):823–827. [PubMed: 2590169]
25. Douglas T, Heinemann S, Bierbaum S, Scharnweber D, Worch H. Fibrillogenesis of collagen types I, II, and III with small leucine-rich proteoglycans decorin and biglycan. Biomacromolecules. 2006 Aug; 7(8):2388–2393. [PubMed: 16903686]
26. Reinboth B, Hanssen E, Cleary EG, Gibson MA. Molecular interactions of biglycan and decorin with elastic fiber components: biglycan forms a ternary complex with tropoelastin and microfibril-associated glycoprotein 1. The Journal of biological chemistry. 2002 Feb 8; 277(6):3950–3957. [PubMed: 11723132]

27. Schonherr E, Witsch-Prehm P, Harrach B, Robenek H, Rauterberg J, Kresse H. Interaction of biglycan with type I collagen. The Journal of biological chemistry. 1995 Feb 10; 270(6):2776–2783. [PubMed: 7852349]
28. Wiberg C, Heinegard D, Wenglen C, Timpl R, Morgelin M. Biglycan organizes collagen VI into hexagonal-like networks resembling tissue structures. The Journal of biological chemistry. 2002 Dec 20; 277(51):49120–49126. [PubMed: 12354766]
29. Yeo TK, Torok MA, Kraus HL, Evans SA, Zhou Y, Marcum JA. Distribution of biglycan and its propeptide form in rat and bovine aortic tissue. Journal of vascular research. 1995 May-Jun;32(3): 175–182. [PubMed: 7772677]
30. Trotter SE, Olsen EG. Marfan's disease and Erdheim's cystic medionecrosis. A study of their pathology. Eur Heart J. 1991 Jan; 12(1):83–87.
31. Collins MJ, Dev V, Strauss BH, Fedak PW, Butany J. Variation in the histopathological features of patients with ascending aortic aneurysms: a study of 111 surgically excised cases. Journal of clinical pathology. 2008 Apr; 61(4):519–523. [PubMed: 17938162]
32. Xu T, Bianco P, Fisher LW, et al. Targeted disruption of the biglycan gene leads to an osteoporosis-like phenotype in mice. Nature genetics. 1998 Sep; 20(1):78–82. [PubMed: 9731537]
33. Lawrence DA. Transforming growth factor-beta: a general review. Eur Cytokine Netw. 1996 Sep; 7(3):363–374. [PubMed: 8954178]
34. Melchior-Becker A, Dai G, Ding Z, et al. Deficiency of biglycan causes cardiac fibroblasts to differentiate into a myofibroblast phenotype. The Journal of biological chemistry. 2011 May 13; 286(19):17365–17375. [PubMed: 21454527]
35. Tang T, Thompson JC, Wilson PG, Nelson C, Williams KJ, Tannock LR. Decreased body fat, elevated plasma transforming growth factor-beta levels, and impaired BMP4-like signaling in biglycan-deficient mice. Connect Tissue Res. 2013; 54(1):5–13. [PubMed: 22834985]
36. Trask BC, Trask TM, Broekelmann T, Mecham RP. The microfibrillar proteins MAGP-1 and fibrillin-1 form a ternary complex with the chondroitin sulfate proteoglycan decorin. Mol Biol Cell. 2000 May; 11(5):1499–1507. [PubMed: 10793130]
37. Corsi A, Xu T, Chen XD, et al. Phenotypic effects of biglycan deficiency are linked to collagen fibril abnormalities, are synergized by decorin deficiency, and mimic Ehlers-Danlos-like changes in bone and other connective tissues. Journal of bone and mineral research : the official journal of the American Society for Bone and Mineral Research. 2002 Jul; 17(7):1180–1189.
38. Boudewijns M, van Dongen JJ, Langerak AW. The human androgen receptor X-chromosome inactivation assay for clonality diagnostics of natural killer cell proliferations. The Journal of molecular diagnostics : JMD. 2007 Jul; 9(3):337–344. [PubMed: 17591933]
39. Bertini E, des Portes V, Zanni G, et al. X-linked congenital ataxia: a clinical and genetic study. Am J Med Genet. 2000 May 1; 92(1):53–56. [PubMed: 10797423]
40. Zanni G, Cali T, Kalscheuer VM, et al. Mutation of plasma membrane Ca2+ ATPase isoform 3 in a family with X-linked congenital cerebellar ataxia impairs Ca2+ homeostasis. Proc Natl Acad Sci U S A. 2012 Sep 4; 109(36):14514–14519. [PubMed: 22912398]

Europe PMC Funders Author Manuscripts

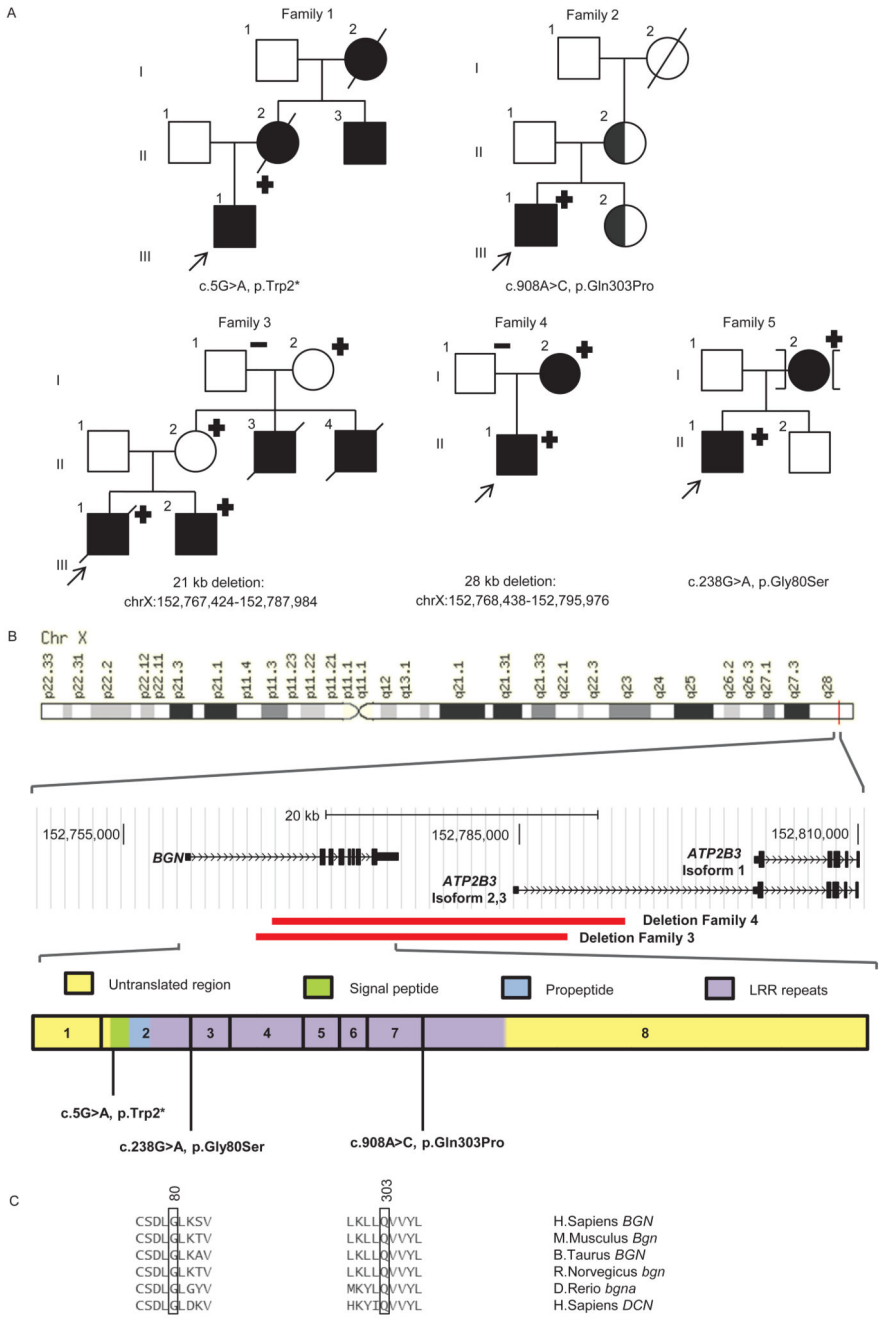

Figure 1. Mutation analysis and *BGN* structure.

(**a**) Pedigrees of the families with their respective mutation. Squares are males, circles females, filled symbols represent aortic aneurysm/dissection and/or systemic involvement; half-filled symbols represent individuals with incomplete clinical data, + or - sign denote presence or absence of BGN mutation. The brackets represent an individual who is adopted into the family.

(**b**) Location of *BGN* on the X-chromosome and identified mutations. Deletions are marked with a red bar. *ATP2B3* isoform 1 represents ENST00000359149. *ATP2B2* isoform 2 and 3 represent ENST00000370186 and ENST00000349466.
(**c**) Conservation of residues on amino acid position 80 and position 303 in other species and in human *DCN*.

Europe PMC Funders Author Manuscripts

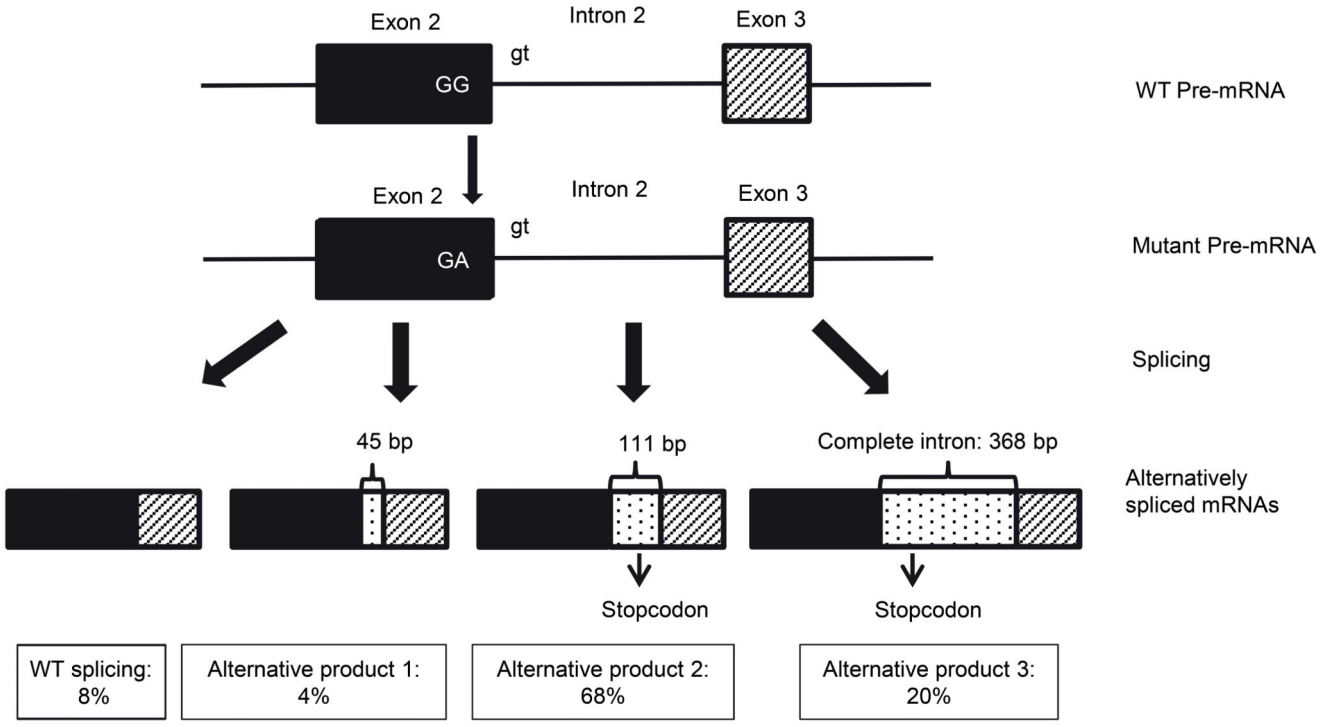

Figure 2. Aberrant splicing in family 5.

In the proband of family 5, three aberrantly spliced mRNAs are produced. The cDNA (converted after inhibition of NMD with puromycin) was cloned into a vector and the number of colonies with the different products were counted (total counted n=94).

Europe PMC Funders Author Manuscripts

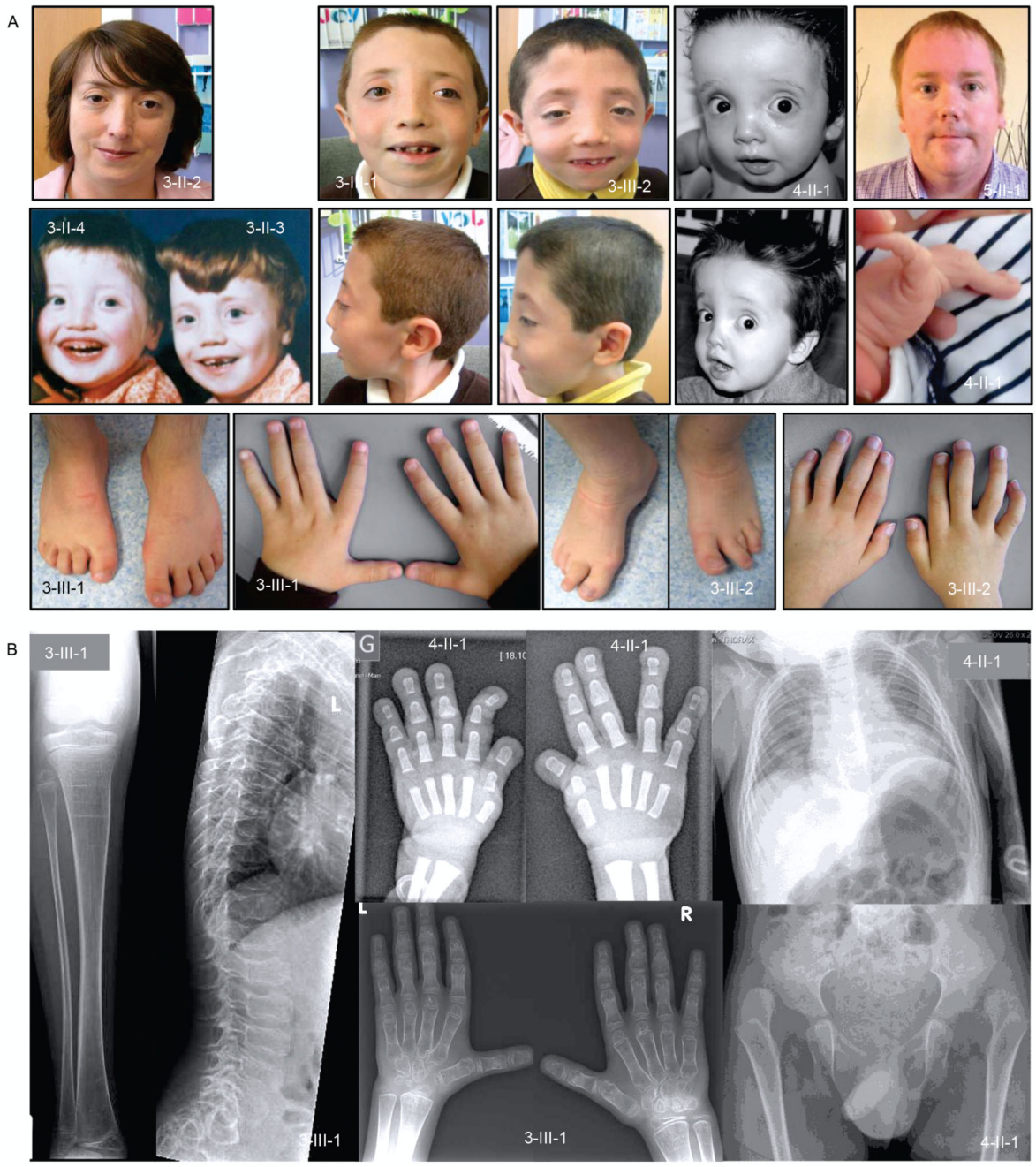

Figure 3. Clinical features.

(**a**) Clinical features include hypertelorism, malar flattening, downslanting palpebral fissures (3-II-2/3/4, 3-III-1/2 and 4-II-1), proptosis (3-III-1/2), joint hypermobility (4-II-1), short, spatulous fingers (3-III-1/2), camptodactyly of fingers and toes (3-III-1/2).

(**b**) Skeletal survey of patient 3-III-1 at age 10 yrs and of patient 4-II-1 at age 1.5 yrs old. Radiograph of both hands (3-III-1) reveals an asymmetry in the size of the carpal bones with the ones on the right side being larger. Overall, there is symmetric shortening and broadening of the metacarpals and phalanges that appear osteopenic with relatively thin

cortices. Lateral view of the spine (3-III-1) demonstrates platyspondyly with at the thoracolumbar transition mild anterior tongueing. Anteroposterior view of the lower limbs (3-III-1) shows that the distal (sub)metaphyseal region of the femur is widened and the knee epiphyses are flattened. There is also mild undermodeling of the tibia with an S-shaped configuration of the diaphysis. The distal tibial epiphysis is dysplastic. Skeletal radiographs of proband 4-II-1 reveal bilateral hip dislocation (treated conservatively), broadened and triangle shaped middle phalanges, broad terminal phalanges and a broad thorax.

Europe PMC Funders Author Manuscripts

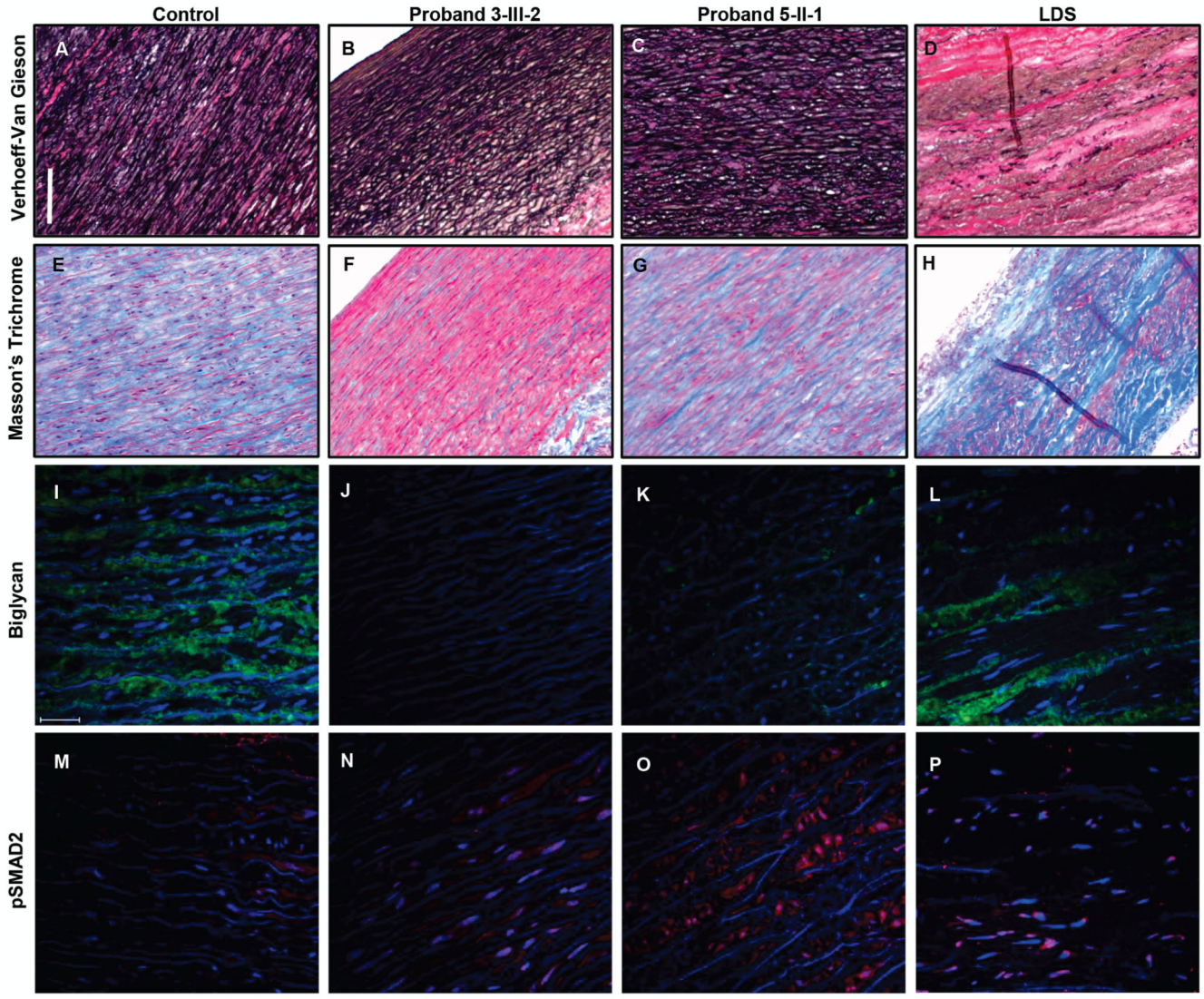

Figure 4. Histological and fluorescent stainings.

(**a-d**) VVG staining of the control sample (**a**), proband 3-III-2 (**b**), proband 5-II-1 (**c**), and an individual with LDS (**d**). The elastin fibers in proband 3-III-2 do not show any clear breaks. In the tissue from the individual with LDS a clear reduction in the elastic fiber content in present. Scale bar indicates 5 mm.

(**e-h**) Trichrome Masson staining of the control sample (e), proband 3-III-2 (**f**), proband 5-II-1 (**g**), and an individual with LDS (**h**). A clear reduction of collagen content is present in proband 3-III-2, while an increase is observed in the individual with LDS.

(**i-l**) Biglycan staining of the control sample (**i**), proband 3-III-2 (**j**), proband 5-II-1 (**k**), and an individual with LDS (**l**). Biglycan is not expressed in proband 3-III-2, while in proband 5-II-1 some residual expression of biglycan is present. In the proband with LDS focal increased expression of biglycan can be observed. Scale bar indicates 25 μm.

(**m-p**) pSMAD2 staining of the control sample (**m**), proband 3-III-2 (**n**), proband 5-II-1 (**o**), and an individual with LDS (**p**). No pSMAD2 positive nuclei are present in the control

sample. In proband 3-III-2, proband 5-II-1 and the proband with LDS an increase in pSMAD2 positive nuclei can be observed.

Europe PMC Funders Author Manuscripts

Europe PMC Funders Author Manuscripts

Table 1

Clinical features

Subject ID	**1-I-2**	**1-II-2**	**1-II-3**	**1-III-1**	**2-III-1**	**3-I-2**	**3-II-2**	**3-II-3**	**3-II-4**	**3-III-1**	**3-III-2**	**4-I-2**	**4-II-1**	**5-I-2**	**5-II-1**	**Freq.**
Age	56†	36†		5	18		44	19†	17†	15†	17	30	2	66	35	
Sex	F	F	M	M	M	F	F	M	M	M	M	F	M	F	M	
Cardiovascular																
Aortic root dilatation	+	+	+	+	+	-	-	+	+	+	+	+	+	+	+	13/15
Aortic dissection	+		-	-	-	-	-	+	-	+	-	-	-	-	-	3/14
Dilated ascending aorta				-	-		-						+		+	2/5
Other					MVP, pulm. art. an.					ASD		AVR	art. tort., PDA an.	brain an.		
Skeletal																
Pectus deformity				+	+		-	-	-	-	-	-	-	-	-	2/11
Arachnodactyly				+	+		-	+	+	-	-	-	-		-	4/10
Brachydactyly							-			+	+	-	-	+	-	3/7
Spatulous fingers							-			+	+	-	+		-	3/6
Flat feet				+	+		-	+	+	-	-	+			-	5/9
Joint hypermobility				+	+		-	+	+	+	+	+	+		-	8/10
Joint dislocation							-		+h	-	-	+s	+h		-	3/7
Joint contracture				+e	+e		-			+f	+f	-			-	4/7
Stature				tall	normal		normal	normal	short	short	short	normal	short	short	normal	
Other									C1/2 spine malf.			scol.				
Craniofacial																
Dolichocephaly					+		-			+	+	-	-		+	4/7
Hypertelorism				-	-		+	+	+	+	+	+	+	+	-	8/11
Down-slanting eyes							+		+	+	+	+	+		-	6/7
Bifid uvula				-	-		-			-	-		+		broad	1/7
High arched palate				+	+		-			-	-					2/5
Proptosis							+	+		+	+	-	-	+	-	5/8
Malar hypoplasia				+			+	+		+	+	-	+		+	7/8
Frontal bossing							-	+	+	+	+	-	+			5/7
Gingival hypertrophy							-					+	+			2/3

Europe PMC Funders Author Manuscripts

Subject ID	1-I-2	1-II-2	1-II-3	1-III-1	2-III-1	3-I-2	3-II-2	3-II-3	3-II-4	3-III-1	3-III-2	4-I-2	4-II-1	5-I-2	5-II-1	Freq.
Cutaneous																
Striae				-	+		-			-	-	+	-	+	+	4/9
Hypertrichosis							-			+	+					2/3
Delayed wound healing							-			-	-	+			-	1/5
Easy bruising							-			-	-	+			-	1/5
Umbilical hernia							-			-	-	-	+		-	1/6
Neurological																
Mild learning problems				+	-		-			-	-					1/5
Dilated cerebral ventricles									+	+			+			3/3
Relative macrocephaly										+	+		+			3/3

Empty cells, not determined. Freq, frequency; †, deceased; M, male; F, Female; MVP, Mitral valve prolapse; pulm. art. an., pulmonary artery aneurysm; ASD, atrial septal defect; AVR, aortic valve regurgitation; art. tort., arterial tortuosity; PDA an., patent ductus arteriosus aneurysm; brain an., brain aneurysm; h, hip; s, shoulder; e, elbow; f, fingers; C1/2 spine malf., C1/2 spine malformation; scol., scoliosis.